Title

Fluid percussion injury device for the precise control of injury parameters

Authors

Wahab, Radia Abdul
Neuberger, Eric J
Lyeth, Bruce G
et al.

Publication Date

2015-06-01

DOI

10.1016/j.jneumeth.2015.03.010

Peer reviewed

Journal of Neuroscience Methods 248 (2015) 16–26

Contents lists available at ScienceDirect

Journal of Neuroscience Methods

journal homepage: www.elsevier.com/locate/jneumeth

Basic Neuroscience

Fluid percussion injury device for the precise control of injury parameters

Radia Abdul Wahab[a], Eric J. Neuberger[b], Bruce G. Lyeth[c], Vijayalakshmi Santhakumar[b], Bryan J. Pfister[a,*]

[a] Department of Biomedical Engineering, New Jersey Institute of Technology, Newark, NJ 07102, United States
[b] Department of Neurology and Neurosciences, Rutgers New Jersey Medical School, Newark, NJ 07103, United States
[c] Department of Neurological Surgery, University of California, Davis, CA 95616, United States

HIGHLIGHTS

- A novel fluid percussion injury (FPI) system was designed and built.
- The system generated fluid percussions with independently adjustable peak pressures, rise times and impulses.
- Immediate post-injury behavior was similar between the custom FPI system and the commonly used FPI system.
- Fluoro-Jade labeling in the hilus and CA2-3 and granule cell population spike amplitude were consistent between systems.
- Slow fluid percussion rise times increased mortality and reduced motor function in a subset of adult rats.

ARTICLE INFO

Article history:
Received 10 December 2014
Received in revised form 5 March 2015
Accepted 6 March 2015
Available online 21 March 2015

Keywords:
Brain injury
Fluid percussion injury
Injury rate
Injury biomechanics

ABSTRACT

Background: Injury to the brain can occur from a variety of physical insults and the degree of disability can greatly vary from person to person. It is likely that injury outcome is related to the biomechanical parameters of the traumatic event such as magnitude, direction and speed of the forces acting on the head.
New method: To model variations in the biomechanical injury parameters, a voice coil driven fluid percussion injury (FPI) system was designed and built to generate fluid percussion waveforms with adjustable rise times, peak pressures, and durations. Using this system, pathophysiological outcomes in the rat were investigated and compared to animals injured with the same biomechanical parameters using the pendulum based FPI system.
Results in comparison with existing methods: Immediate post-injury behavior shows similar rates of seizures and mortality in adolescent rats and similar righting times, toe pinch responses and mortality rates in adult rats. Interestingly, post injury mortality in adult rats was sensitive to changes in injury rate. Fluoro-Jade labeling of degenerating neurons in the hilus and CA2-3 hippocampus were consistent between injuries produced with the voice coil and pendulum operated systems. Granule cell population spike amplitude to afferent activation, a measure of dentate network excitability, also showed consistent enhancement 1 week after injury using either system.
Conclusions: Overall our results suggest that this new FPI device produces injury outcomes consistent with the commonly used pendulum FPI system and has the added capability to investigate pathophysiology associated with varying rates and durations of injury.

1. Introduction

Each year an estimated 1.7 million Americans and 10 million people worldwide sustain a traumatic brain injury (TBI). Worldwide, TBI is predominate in low to middle income countries which may relate to increased risk factors and availability of medical treatment (Faul et al., 2010; Hyder et al., 2007). Considering all cases of TBI, the degree of disability can vary greatly from person to person. TBI can occur from a variety of physical insults to the brain such as an automobile accident, sport collision or blast wave. Indeed, it is likely that the wide range of TBI outcomes may be due to the biomechanics of the traumatic event such as magnitude, direction and speed of the forces acting on the head. A majority of TBI

* Corresponding author at: Department of Biomedical Engineering, New Jersey Institute of Technology, University Heights, Newark, NJ 07102, United States.
E-mail address: pfister@njit.edu (B.J. Pfister).

http://dx.doi.org/10.1016/j.jneumeth.2015.03.010
0165-0270/

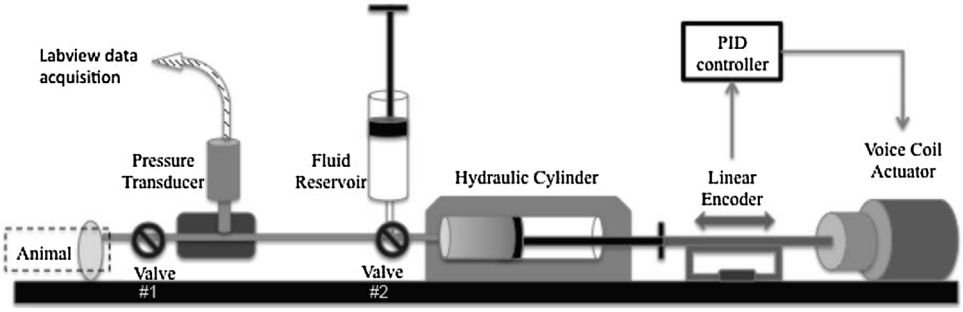

Fig. 1. Programmable fluid percussion injury system. A voice coil linear actuator drives a hydraulic cylinder to produce a fluid percussion. A PID closed loop control system uses encoder feedback to program specific movements that translate into definable fluid percussion waveforms. A pressure transducer is located near the animal connection to measure the fluid percussion applied.

studies link the magnitude of the primary injury (i.e. peak pressure in the fluid percussion model) to severity in terms of brain pathology and behavioral outcomes. The contributions that the temporal characteristics of the injury such as rise time and duration have on damage to the brain have just begun to be investigated (Cater et al., 2005; Magou et al., 2011; Ganpule et al., 2013; Sundaramurthy et al., 2012).

In closed head injury, damage to axons is thought to be induced by deformation of the brain tissues in response to an insult (Smith and Meaney, 2000; Meaney et al., 1995). Lateral fluid percussion brain injury (FPI) is one of the most commonly used and well-characterized experimental models of TBI. It is used to deform the brain of rodents to produce both focal and diffuse injury characteristics (Cortez et al., 1989; Dixon et al., 1987; Graham et al., 2000; Hicks et al., 1996; Morales et al., 2005; Thompson et al., 2005). Potentially, one of the biggest contributors to differences in TBI outcome could be the rate at which pressure changes in addition to magnitude of pressure that deforms the brain (Magou et al., 2011; Ganpule et al., 2013; Sundaramurthy et al., 2012). The term "rate" is defined as the rise time to peak pressure. Because brain tissue is viscoelastic, both rate and magnitude of the pressure will affect how the tissue responds mechanically and thus could lead to unique pathophysiologies (Magou et al., 2011; Shuck and Advani, 1972; Arbogast et al., 1997). Greatly contrasting examples would be a head impact from a fall vs. a blast wave; the latter being several order of magnitude higher in rate.

The contribution of the rate of injury was recognized in early head injury physical models (Sundaramurthy et al., 2012; Shuck and Advani, 1972; Arbogast et al., 1997; Smith et al., 1997; Liu et al., 1975; Adams et al., 1983; King et al., 2003), where injury was correlated with rotational acceleration of the head. Currently, there are no animal models directly examining whether the pathophysiological outcome of injury depends on the rate of the delivered injury. This is likely due to the limitations of the available animal models to only adjust for injury magnitude. For instance, FPI and weight drop injury vary either by height adjustment of the pendulum in FPI (Dixon et al., 1987; McIntosh et al., 1989) or by height or mass adjustment of the dropped weight (Dail et al., 1981; Feeney et al., 1981; Marmarou et al., 1994; Sawauchi et al., 2003). A notable exception, the miniature pig injury model, can adjust rotational acceleration. In this model the device rapidly rotates the animal's head over the designated angular excursion at specific angular accelerations, which correlated with severity of diffuse brain trauma (Smith et al., 1997). The model, however, is difficult to replicate and not widely used.

In this study we have developed a computer controlled FPI device based off the widely used animal model. Using a voice coil actuator to drive the fluid percussion, this system can generate a desired pressure waveform including independent control of injury rise time and duration. Here we characterized the system capabilities and verified it against a commonly used FPI device.

2. Methods

2.1. Computer controlled fluid percussion device

A voice coil actuator driven fluid percussion injury system (vcFPI) was developed to precisely control the characteristics of the pressure waveform including rise time and peak pressure. Fluid percussions were generated by moving a rigidly connected hydraulic cylinder with a linear voice coil actuator (LA2-42-000A, BEI Kimco) (Fig. 1). Accordingly, the controlled motion of the voice coil and hydraulic cylinder translates into a controlled rise in fluid pressure. A flat-faced pressure transducer (px61v0-100gv, Omegadyne) was mounted at the output of the hydraulic cylinder to measure the applied fluid percussion. A 2.6 mm-ID female Luer-loc fitting connected the injury device to a male Luer-loc connector cemented to the rat skull. LabView (National Instruments) was used to acquire the fluid percussion pressure waveform for analysis.

The movement of the voice coil actuator was controlled by a proportional-integral-derivative (PID) controller (Pfister et al., 2003) (S100, Automation Modules) (Fig. 1). A linear optical encoder (Zeiss, LEI 5, 1 μm resolution) was used to close the PID control loop. Voice coil hydraulic cylinder motion was programmed to make a desired, target displacement using a triangular motion scheme. A triangular motion refers to the velocity profile of the motion at a constant acceleration. The desired or target motion is determined by the equation of motion and the programmed velocity and acceleration. The optimum values for displacement and velocity leading to the desired pressure pulse were determined experimentally. Displacement was varied to control the desired peak pressure. Velocity was chosen to achieve the desired rate of rise. A constant acceleration was specified at the maximum value for a linear rise in the pressure.

2.2. Characterization of pressure waveform generation

Motion control is affected by the physics of the system including the mass and friction of the moving parts and the compliance of the load attached to the hydraulic cylinder (i.e. a rat head). To characterize the motion control of the mechanical system without the presence of a load, valve #1 was closed creating a non-compliant system (Fig. 1). A span of displacements was executed and the resulting pressure was recorded. Pressure pulse data was analyzed to determine peak pressure, rise time, and impulse. Rise time was calculated as the pressure rise from 10% increase to 90% of the peak representing the rate at which the injury was delivered. The impulse of the pressure waveform is a representation of the total energy transferred to the brain tissues and was calculated as the

area under the pressure pulse recording using the following formula:

$$I = \sum_{t=s}^{e} P(t)$$

where "I" is the impulse (units Pa s), "$P(t)$" is the pressure waveform, "$t = s$" is the start of the positive pressure region, "$t = e$" is the end of the positive pressure region.

2.3. Lateral fluid percussion injury

Standard surgical methods for lateral fluid percussion injury were followed for 26-day-old adolescent rats (Gupta et al., 2012; Santhakumar et al., 2003) and 3-month-old adult rats (Lyeth et al., 1990; Zhao et al., 2003). Briefly, adolescent rats were anesthetized with ketamine (80 mg/kg)/xylene (10 mg/kg), i.p. whereas the adult rats were mechanically ventilated (model 683; Harvard Apparatus, Hollister, MA) with 2% isoflurane in a 2:1 nitrous oxide/oxygen carrier gas. All rats were mounted on a stereotaxic device (model 900; KOPF Instruments, Tujunga CA) and a craniectomy (diameter of 4.8 mm for adult rats and 2.5 mm for adolescent rats) was performed on the parietal bone (centered at −4.5 mm Bregma, 3 mm lateral, for adult rats; and, 3.5 mm for adolescent rats). A Luer-loc needle hub was set over the opening with cyanoacrylate adhesive and then secured to the skull with cranioplastic cement (Plastic One, Roanoke, VA) and two skull screws placed into burr holes, 1 mm rostral to Bregma and 1 mm caudal to Lambda. Rectal temperature was continuously monitored and maintained within normal ranges during surgical preparation by a feedback temperature controller pad (model TC-1000; CWE Ardmore, PA).

Forty-five adolescent male Wistar rats (Charles River, Indianapolis, IN), 35–65 g and eighty-one adult Sprague-Dawley rats (Harlan), 300–350 g were used for this study. Standard experimental TBI was induced using the commonly used pendulum FPI (pFPI) system (Custom Design and Fabrication, VCU Biomedical Engineering, Richmond, VA) and compared to our vcFPI system on separate sets of animals. Animals were handled in accordance with the Public Health Service (PHS) Policy on Humane Care and Use of Laboratory Animals. All protocols were approved by the Rutgers Institutional Animal Care and Use Committee (adolescent rats) and University of California at Davis Institutional Animal Care and Use Committee (adult rats).

2.4. Post-injury pathophysiology and anatomy

Adolescent animals were not ventilated after the injury and were observed for 15 min for the development of seizures. Seizures were identified by muscle stiffening or sudden cessation of activity followed by uncontrolled jerking or spasms.

Adult rats were ventilated after injury with air in the absence of isoflurane. As soon as spontaneous breathing was observed righting reflex and toe pinch tests were performed. The righting reflex was assessed by placing the rat in a supine position at regular intervals (~30 s) to test the rat's ability to spontaneously recover to a prone position. The toe pinch response was assessed at regular interval (~15 s) by firmly pinching the hind paw toes to elicit a paw withdrawal response.

2.5. Neuronal degeneration

Fluoro-Jade labeled neuronal degeneration was assessed at 4 h for adolescent rats and 24 h for adult rats after FPI (Schmued and Hopkins, 2000). Rats were anesthetized (sodium pentobarbital, 70 mg/kg, i.p.) and transcardially perfused with 0.1 M phosphate buffered saline (PBS) for 2 min followed by 4% paraformaldehyde for 5 min. Brains were extracted and cut into 45 μm thick slices using a vibratome (Leica Microsystems, VT1200S) for adolescent rat tissues, and a sliding microtome (model #860, American Optical Corporation, Buffalo, NY) for adult rat tissues. A minimum of 4 randomly selected sections from septal and temporal poles and mid-levels of hippocampus on the injured side were examined to identify the presence and distribution of Fluoro-Jade C staining. Tissue sections were mounted on gelatin-coated slides in 0.1 M PBS and distilled H_2O at 1:1 ratio and air-dried overnight. The slide-mounted tissue sections were subsequently immersed in 100% alcohol (3 min), 70% alcohol (1 min), dH_2O (1 min), and 0.006% potassium permanganate (15 min). Sections were rinsed in dH_2O (1 min), incubated in 0.001% Fluoro-Jade B (FJ-B) (Histo-Chem Inc., Pine Bluff, AK) staining solution in 0.1% acetic acid for 30 min, rinsed again in H_2O (3 min), and air-dried. Finally, the sections were immersed in xylene and cover-slipped with DePeX mounting medium (Electron Microscopy Sciences, Fort Washington, PA).

2.6. Electrophysiology

1-week post injury, adolescent rats were anesthetized with 1–3% isoflurane, decapitated, brains removed, and cooled to 4 °C in oxygenated sucrose-aCSF (artificial cerebrospinal fluid with 95% O_2 and 5% CO_2 at pH 7.4)(Gupta et al., 2012; Yu et al., 2013). Brains were cut into 400 μm horizontal brain slices using a vibratome (Leica, VT1200S), sagittally bisected into two hemispherical components (ipsilateral and contralateral to the injury site) and held at room temperature in oxygenated aCSF. Individual slices were transferred to an interfaced recording chamber (BSC2, Automatic Scientific), and perfused with oxygenated recording-aCSF (Gupta et al., 2012; Yu et al., 2013).

Field recordings were performed in the granule cell layer of the dentate gyrus by using patch pipettes (4 MΩ, KG-33 borosilicate glass capillary with 1.5 mm outer diameter from Harvard Apparatus, pulled using a Sutter P-1000 horizontal micropipette puller) filled with recording-aCSF as in earlier studies (Gupta et al., 2012; Yu et al., 2013; Neuberger et al., 2014). Responses were evoked by constant-current stimulation of the perforant path fibers (4 mA, 50 μs) delivered at 0.1 Hz through custom made, parallel bipolar 90-μm tungsten stimulating electrode placed in the junction of the dorsal blade and the crest as previously described (Gupta et al., 2012; Yu et al., 2013; Neuberger et al., 2014). Recordings were obtained from granule cell layer of the dentate gyrus with an AxoPatch 200B amplifier and digitized at 10 kHz with DigiData 1440A (Molecular Devices, Sunnyvale, CA). The population spike was measured as the amplitude of the first negative deflection overriding the field excitatory post-synaptic potential (EPSP) waveform as described previously (Neuberger et al., 2014; Santhakumar et al., 2001).

2.7. Statistical analysis

Data analysis was performed using SPSS software (version 17, Chicago, IL) and a general linear model was used for analysis. The alpha level was set to 0.05 for rejecting nulls hypothesis. Data for pressure peaks, rise times and impulse were expressed as mean ± standard error of mean (SEM) and analyzed using one-way analysis of variance (ANOVA) followed by Bonferroni where appropriate.

All other animal data (seizure rates, righting times and toe pinch response, electrophysiology) were expressed as mean ±SEM. Significance was tested by Student's t-test and chi-square test for comparing two sets of data where appropriate.

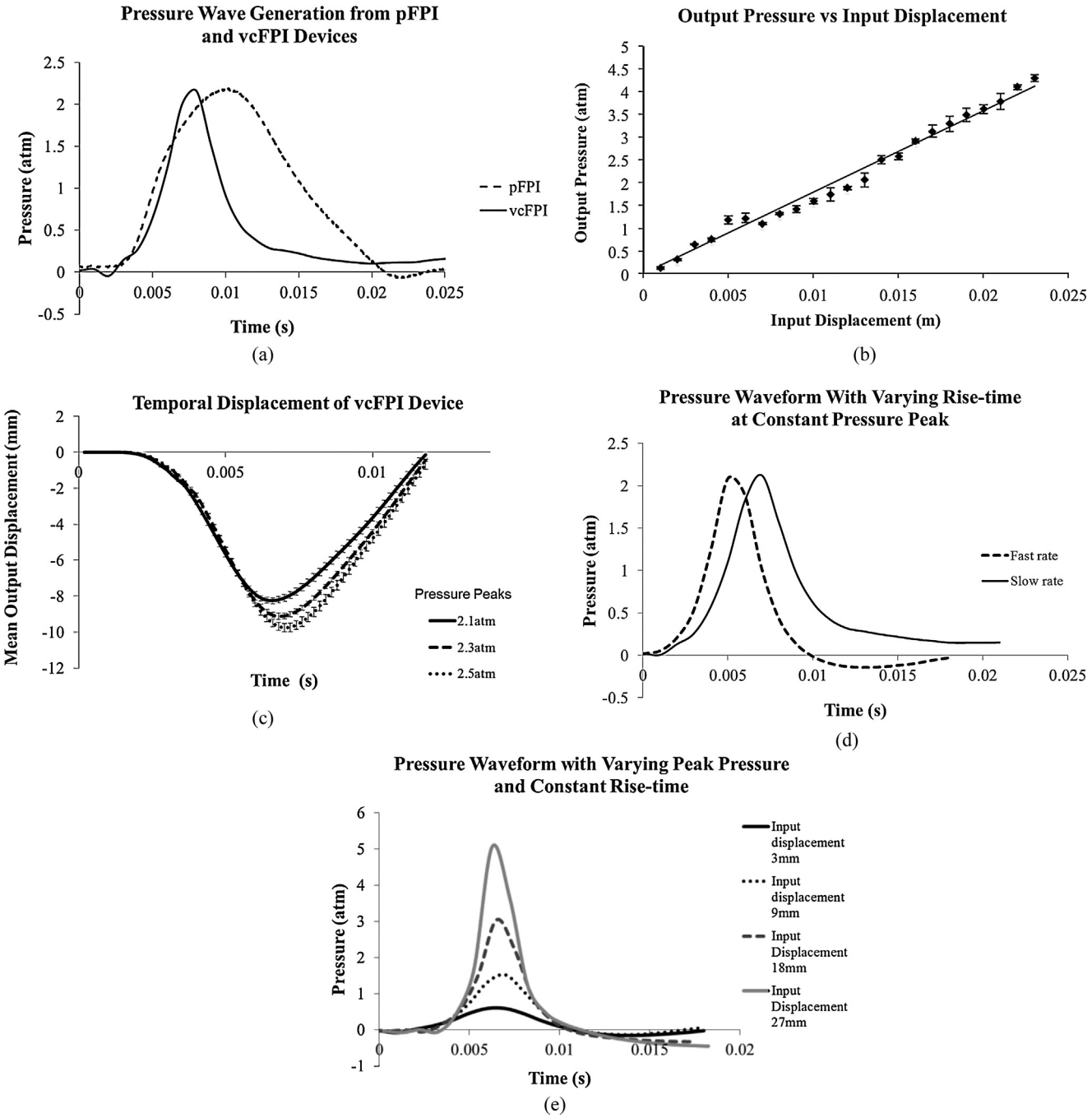

Fig. 2. Closed system device characterization. (a) Output pressure waves generated by pFPI and vcFPI device. (b) Input vs. output characteristics of the vcFPI system. For a range of input displacements from 0.001 m to 0.023 m, the output pressure peaks were recorded and the results showed a linear system response ($n = 3$, $R^2 = 0.99$). (c) Voice coil motion resulting from 3 different peak pressures ($n = 4$). Peak displacements were 8.25 ± 0.16 mm, $9.12 \pm 0.0.16$ mm, 9.76 ± 0.22 mm corresponding to peak pressures 2.1 atm, 2.3 atm and 2.5 atm respectively. (d) Comparison of pressure waveforms of two different rates of rise-time (fast-rise: 2.89 m/s and slow-rise: 3.36 m/s) at constant peak pressures using the vcFPI system. (e) Comparison of pressure waveforms by varying input displacements and keeping rise-time constant. (d) and (e) illustrate that the vcFPI device is capable of independently varying rise-time and peak pressure.

3. Results

3.1. Voice coil motion–pressure waveform characterization

To produce a controlled fluid percussion, a closed system was evaluated to adjust and optimize the gain settings of the PID control (valve #1 closed; Fig. 1). The closed system eliminated potential variability from loads connected outside the system (i.e. an animal). Fluid percussions were generated from closed systems and compared between both the pFPI system and vcFPI system. The vcFPI system produced fluid percussions similar to the pFPI device as well as more rapid percussions while maintaining peak pressure (Fig. 2a).

Since the system is motion control based, programmed voice coil–hydraulic cylinder displacement was mapped to the pressure waveform output. Using the closed system as above, a range of displacements from 0.001 m to 0.023 m was programmed at a velocity of 3.36 m/s and acceleration of 1502 m/s^2. The peak pressures produced were linearly related to displacement of the hydraulic cylinder (Fig. 2b) ($n = 3$, $R^2 = 0.99$). The small standard deviations indicate the repeatability of fluid percussion pressures generated by the device. Temporal consistency of motion control

is also important to the creation of a controlled fluid percussion. Fig. 2c plots voice coil motion for three displacements, which create fluid percussions in the moderate injury range ($n = 4$ for each displacement). Importantly, all the three displacement curves showed similar acceleration and velocity, each reaching their respective displacements. Resultant mean displacements were 8.25 ± 0.16 mm, 9.12 ± 0.16 mm and 9.76 ± 0.22 mm corresponding to peak pressures of 2.10 ± 0.06 atm, 2.48 ± 0.06 atm and 2.57 ± 0.04 atm respectively.

Since voice coil motion is directly coupled to the hydraulic cylinder, increasing voice coil velocity results in pressure waveforms with faster rise-times and keeping displacement constant maintains the same peak pressure. Motions were programmed to produce a displacement resulting in peak pressures of 2.15 atm at two different velocities 2.89 m/s and 3.36 m/s (Fig. 2d). The two resulting pressure waveforms had consistent peaks with increasing rise-times. Likewise, increasing voice coil displacement (input displacement in mm: 3, 9, 18, 27), keeping velocity constant, resulted in pressure waveforms with different pressure peaks with constant rise-times (Fig. 2e).

3.2. Variation with pendulum FPI model

Our goal was to develop a programmable FPI device in order to study the effects of pressure rise time on physiological effects of injury to the brain. Accordingly, the vcFPI device was programmed to operate at faster rise times than the pFPI device. The vcFPI and pFPI systems were operated under the closed configuration (valve #1 closed) and the peak pressure, rise time, and impulse were analyzed. For comparison, three pressure waveforms were produced: a fluid percussion magnitude of 2.15 atm with the pFPI device, a fast pressure waveform with the vcFPI system using the maximum velocity of 3.36 m/s at an acceleration of 1502 m/s^2, and a slower waveform with the vcFPI at a velocity of 2.89 m/s at an acceleration of 1420 m/s^2.

The vcFPI system was programmed such that the three peak pressures were nearly identical [2.14 ± 0.002 atm for pFPI ($n = 10$), 2.15 ± 0.033 atm for fast vcFPI ($n = 10$) and 2.15 ± 0.015 atm for slow vcFPI ($n = 10$); Fig. 3a] with no significant differences between groups [$F(2,27) = 0.059$, $P \cong 1$]. The rise-times for each waveform were different: 5.3 ± 0.09 ms for pFPI, 3.1 ± 0.05 ms for fast vcFPI injury and 4 ± 0.15 ms for slow vcFPI (Fig. 3b). One-way ANOVA between groups revealed that the rise times were significantly different between groups [$F(2,27) = 121$, $P < 0.05$]. The impulse for the pFPI was the highest (2052 ± 33 Pa s), the fast vcFPI injury was the least (762 ± 11 Pa s) and the slow vcFPI was 1086 ± 8 Pa s (Fig. 3c). One-way ANOVA revealed that the impulse between the three groups were significantly different [$F(2,27) = 1057$, $P < 0.05$].

3.3. Generation of fluid percussions with load

Pressure waveforms generated by an open system with valve #1 open and a compliant load (i.e. rat brain) on the system. Two different age groups of rats commonly used in FPI studies (26-day-old adolescent and 3-month-old adult) were evaluated with the pFPI and vcFPI devices. Moderate injury peak pressures were chosen for analysis; 1.77 atm for adolescent rats and 2.15 atm for adult rats.

For adolescent rat injuries, the vcFPI system was programmed to create a fluid percussion similar to the pFPI device (slow vcFPI). In addition, the vcFPI system was programmed to create a faster fluid percussion at the same pressure magnitude (Fast vcFPI) (Fig. 4a). Peak pressures were 1.67 ± 0.03 atm for pFPI ($n = 9$), 1.77 ± 0.04 atm for slow vcFPI ($n = 17$) and 1.82 ± 0.11 atm for fast vcFPI ($n = 20$) and were not significantly different between the groups [$F(2,43) = 0.6$, $P \cong 1$] (Fig. 5a). Rise-times were 8.2 ± 0.2 ms ($n = 9$) for pFPI, 8.7 ± 0.4 ms ($n = 17$) for slow vcFPI and 3.1 ± 0.1 ms

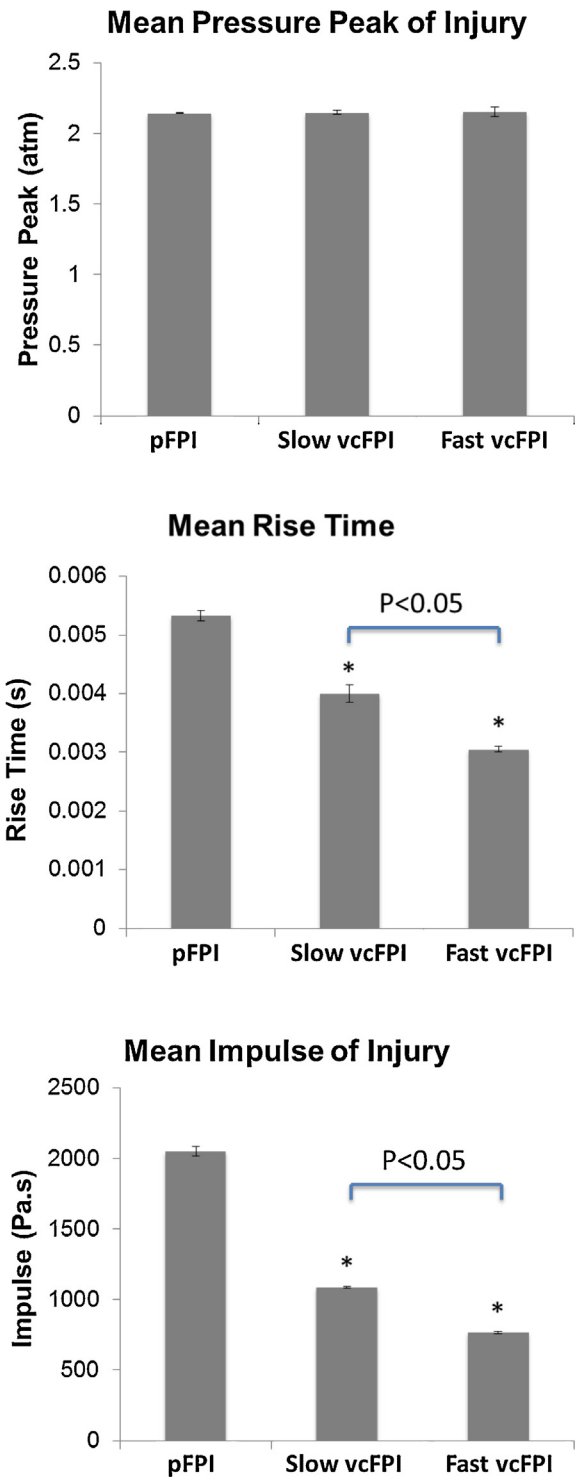

Fig. 3. Pressure waveform analysis of a closed system. Mean values were compared between commonly used pFPI system and fast-rise using the vcFPI and slow rise also using the vcFPI system. (a) Mean peak pressures, (b) mean rise-times, and (c) mean impulse (area under the pressure–time curve). Standard error bars shown in (a), (b) and (c). *Indicates significant differences (Bonferroni) vs. pFPI.

($n = 20$) for fast vcFPI (Fig. 5b). One-way ANOVA between groups [$F(2,43) = 135.9$, $P < 0.001$] and Bonferroni post hoc analysis indicated that rise-time for pFPI and slow vcFPI were not different while fast vcFPI had a significantly lower rise time than both pFPI and slow vcFPI. The impulse for adolescent rat injuries were 2121 ± 61 Pa s ($n = 9$) for pFPI, 1940 ± 86 Pa s ($n = 17$) for slow vcFPI and 979 ± 36 Pa s ($n = 20$) for fast vcFPI (Fig. 5c). One-way

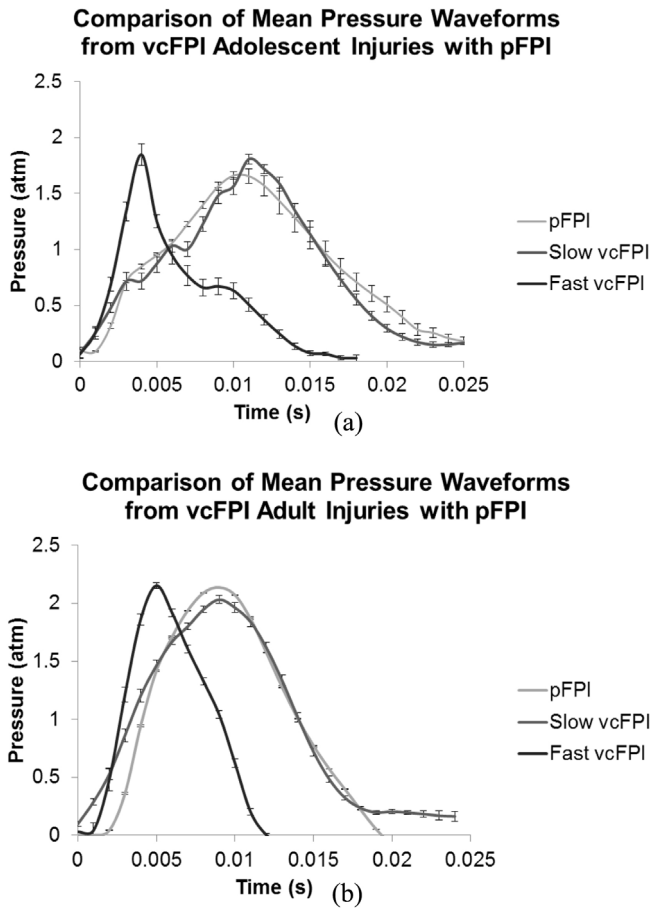

Fig. 4. Representative pressure waveforms in (a) adolescent and (b) adult rats from injuries: fast vcFPI, slow vcFPI and the pFPI. The graphs show fast vcFPI waveforms have shorter rise-time than slow vcFPI waveforms in both adult and adolescent animals. The graphs also show that the slow vcFPI setting produced a waveform very similar to the pFPI waveform in both adolescent rats and adult rats. Error bars represent SEM.

ANOVA [$F(2,43) = 93.05$, $P < 0.001$] and Bonferroni post hoc analysis revealed significant difference in the impulse between the three waveforms. Since there was no difference between the pressure peak and the rise time of pFPI and slow vcFPI, the difference in the impulse between these two groups may be due to differences in decay time.

For adult rat injuries, we considered a slightly wider variation in injury rise times from the pFPI device. Here, the vcFPI system was programmed to create fluid percussions slower (slow vcFPI) and faster (fast vcFPI) than the pFPI with the goal of keeping the pressure magnitude constant (Fig. 4b). Peak pressures were 2.15 ± 0.004 atm, $n = 29$ for pFPI, 1.98 ± 0.03 atm, $n = 31$ for slow vcFPI, and 2.15 ± 0.02 atm, $n = 19$ for fast vcFPI (Fig. 5a). There was a small (0.17 atm) but statistically significant difference between the peak pressure of slow vcFPI and fast vcFPI peaks [$F(2,59) = 17.24$, $P < 0.05$]. Rise times were 6.2 ± 0.07 ms ($n = 13$) for pFPI, 7.8 ± 0.14 ms ($n = 31$) for slow vcFPI, 3.0 ± 0.12 ms ($n = 19$) for fast vcFPI (Fig. 5b). One-way ANOVA [$F(2,59) = 215.2$, $P < 0.05$] and Bonferroni post hoc analysis revealed that the rise-times were significantly different between all three groups. Finally, impulse was 2059 ± 13 Pa s ($n = 13$) for pFPI, 2198 ± 33 Pa s ($n = 31$) for slow vcFPI, and 1214 ± 25 Pa s ($n = 19$) for fast vcFPI (Fig. 5c). One-way ANOVA [$F(2,59) = 292.4$, $P < 0.05$] and Bonferroni post hoc analysis revealed that the impulses were significantly different between all three groups. Therefore the 3 different groups were injured with pressure waves with distinct rise-time and impulse, at similar pressure peak.

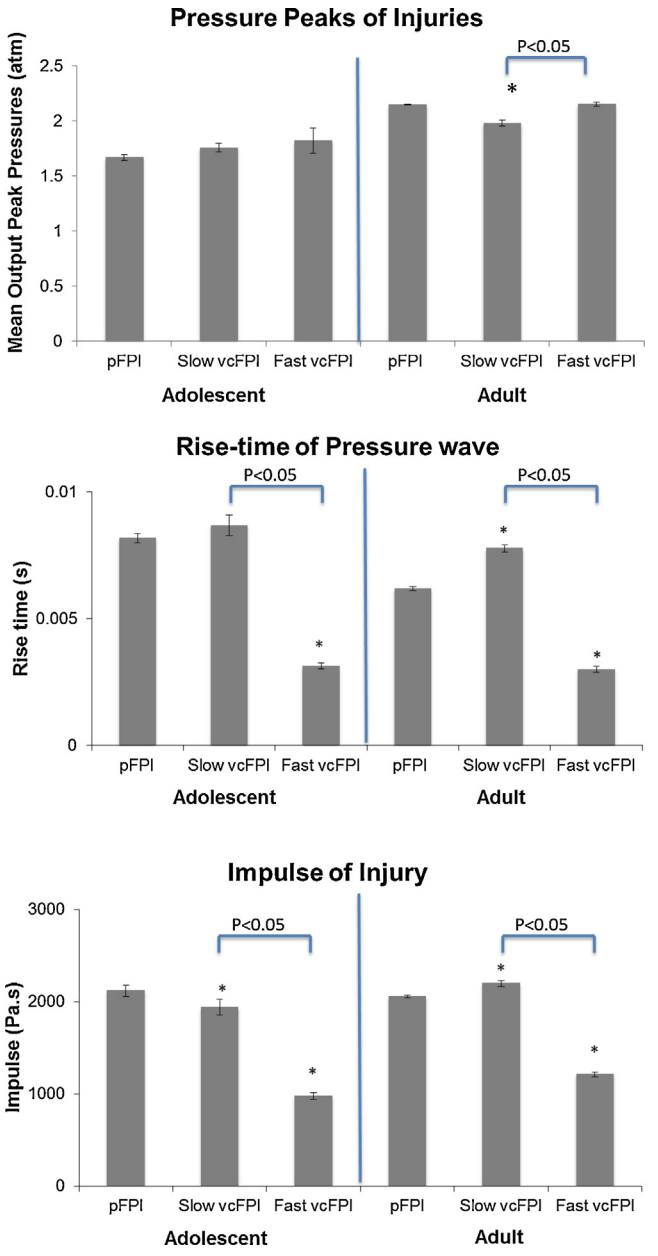

Fig. 5. Waveform analysis from adolescent and adult injuries. Mean (a) peak pressures, (b) rise-times and (c) impulse from adolescent and adult rats for pFPI injuries, fast and slow vcFPI injuries were compared. For adolescent rats the target pressure peak for a moderate injury was 1.77 atm and that for adult rats was 2.15 atm. Standard error bars shown in (a), (b), and (c). *Indicates significance by ANOVA and Bonferroni post hoc analysis comparing groups to pFPI group of the same age group.

3.4. Injury induced pathophysiology

Fluid percussion injury commonly induces seizures and a small percentage of death in adolescent rats (Neuberger et al., 2014). Here we compared the instance of seizure and death from injury with both FPI systems using similar fluid percussions: rise times were 8.2 ± 0.19 ms for pFPI and 8.75 ± 2.1 ms for vcFPI ($P > 0.05$, by Student's t-test); peak pressures were 1.67 ± 0.03 atm for pFPI and 1.84 ± 0.12 atm for vcFPI ($P > 0.05$); and impulses were 2121 ± 38 Pa s for pFPI and 2025 ± 535 Pa s for vcFPI ($P > 0.05$).

A similar number of rats injured with the vcFPI demonstrated post-injury seizures compared to those injured by the pFPI device (vcFPI: 74%, $n = 19$; pFPI: 70%, $n = 20$, $P > 0.05$ by Chi-square test;

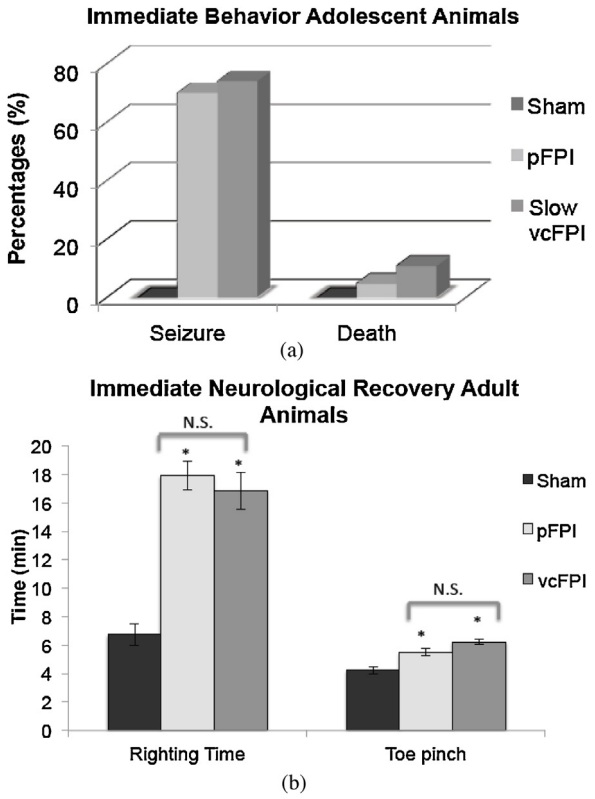

Fig. 6. Fluid percussion injury assessment: immediate behavioral assessment in (a) adolescent animal group seizure and mortality rate, (b) adult animal group righting time and toe pinch response. *Indicates significant differences (Bonferroni) vs. Sham.

Fig. 6a). The percentage of rats that died at injury was also not significantly different between the vcFPI and pFPI groups (vcFPI: 11%, $n = 19$; pFPI = 5%, $n = 20$, $P > 0.05$ by Chi-squared test; Fig. 6a). Sham TBI rats suffered no seizures or death ($n = 7$). This shows that the two devices performed similar immediate effects in terms of seizure and mortality rates.

For adult rats, righting time and toe pinch are common immediate measures used to determine injury from a fluid percussion (Lyeth et al., 1990). Here, adult rats were injured with both FPI systems at different injury rise times keeping pressure and impulse constant. Fluid percussion rise times were 6.1 ± 0.3 ms for pFPI ($n = 3$), 8.7 ± 0.45 ms for slow vcFPI ($n = 7$) ($P < 0.05$, by Student's t-test), peak pressures were 2.15 ± 0.002 atm for pFPI ($n = 6$) and 1.93 ± 0.06 atm for slow vcFPI ($n = 7$) ($P < 0.05$), and impulses were 2014 ± 8 Pa s for pFPI ($n = 3$) and 2121 ± 58 Pa s for slow vcFPI injuries ($n = 7$) ($P > 0.05$). Despite differences in injury rise times, animals injured from both systems had very similar righting times and toe-pinch response times. Righting times were 18 ± 1.0 min ($n = 6$) for pFPI, 17 ± 1.2 min ($n = 7$) for vcFPI, and 7 ± 0.8 min ($n = 2$) for sham animals ($P > 0.05$, by Student's t-test) (Fig. 6b). Toe-pinch response times were 5.5 ± 0.3 min ($n = 6$) for pFPI, 6.2 ± 0.2 min ($n = 7$) for slow vcFPI, and 4.3 ± 0.4 min ($n = 2$) for sham ($P > 0.05$, t-test). Results from one-way ANOVA (including sham group) revealed significant difference from sham in righting time by group [$F(2,12) = 11.58$, $P < 0.05$] and toe pinch response by group [$F(2,12) = 9.91$, $P < 0.05$].

The effect of injury rise-time was further considered from a larger adult animal group between: pFPI injured, slow vcFPI injured and fast vcFPI injured with pressure and impulse constant. Slow and fast refer to rise-times slower and faster than the pFPI (see Table 1). Animals were pooled from a separate cohort of injuries in our laboratory studying rise time related behavioral deficits post injury; where the mortality rate presented here was not considered

Table 1
Effect of rise time on injury outcome in adult rats.

	Sham	pFPI	Slow vcFPI	Fast vcFPI
Rise-time (ms)	0	6 ± 0.07	8 ± 1.4	3 ± 1.1
Total injuries	16	27	31	21
Immediate deaths	0	3	11	0
Non-functional eliminated	0	0	3	0
Animal elimination rate	0%	11%	45%	0%

elsewhere. Overall, the fast vcFPI produced no mortality unlike the slower groups. Slow vcFPI ($n = 31$) produced 45% mortality, pFPI ($n = 29$) produced 10% mortality and fast vcFPI ($n = 19$) produced no mortality ($P < 0.05$ by Chi-squared test). Interestingly, 3 surviving animals in the slow vcFPI group could not physically perform behavioral tasks and were eliminated from study. Less than 4% of adult rats injured demonstrated post-injury seizures. No seizures or death were observed in Sham TBI rats ($n = 16$). This suggests that fluid percussions of similar magnitude but differing rate may lead to differences in post injury outcome.

3.5. Neuronal degeneration and altered electrophysiological function

Animals injured using both FPI systems were evaluated for neuronal degeneration and altered electrophysiological function. Neuronal degeneration was assessed at 4 h post injury for adolescent rats and at 24 h for adult rats. The hilus region of the hippocampus in adolescent rats animals showed quantitatively similar cellular degeneration in slices from in both pFPI and vcFPI injured animals. The sham animals showed no apparent cellular degeneration. Similar to the adolescent rat brain tissue slices, the CA3 region of the adult rats showed quantitatively similar cellular degeneration from injuries using both systems. The sham animals showed no apparent cellular degeneration (Fig. 7a).

Earlier studies have shown that FPI causes an early increase in afferent-evoked dentate network excitability 1 week after injury due to changes to both excitatory and inhibitory network function (Gupta et al., 2012; Santhakumar et al., 2001, 2003; Lowenstein et al., 1992; Toth et al., 1997). Here we examined the granule cell population response to perforant path activation in slices from animals injured using the pFPI and vcFPI device 1-week post injury. The perforant path was stimulated with 4 mA and EPSPs were recorded in the granular cell layer of the dentate gyrus. EPSPs in pFPI and vcFPI injured rats produced population spikes resulting in the expected injury induced hyperexcitability. Evoked granule cell population spike amplitude in both groups of injured animals were the same (in mV): sham: 0.001 ± 0.00 ($n = 4$ slices for 4 rats); pFPI: 1.36 ± 0.38 ($n = 7$ slices from 4 rats; part of this data has been published in Gupta et al., 2012); vcFPI: 0.81 ± 0.25 ($n = 4$ slices from 4 rats). Sham-TBI rats did not produce population spikes (Fig. 7b). One way ANOVA between groups show a significant difference between groups in population spike amplitude [$F(2,14) = 4.10$, $P < 0.05$]. Post hoc Bonferroni test reveals that there was no significant difference between the pFPI group and vcFPI group. The similar enhancement in dentate excitability 1 week after injury using either device shows that both devices induce similar physiological pathology.

4. Discussion

Lateral fluid percussion injury is one of the most commonly used and well-characterized experimental models of TBI (Morales et al., 2005; Thompson et al., 2005). Here, a voice-coil driven fluid percussion injury device (vcFPI) was designed and built to model TBI

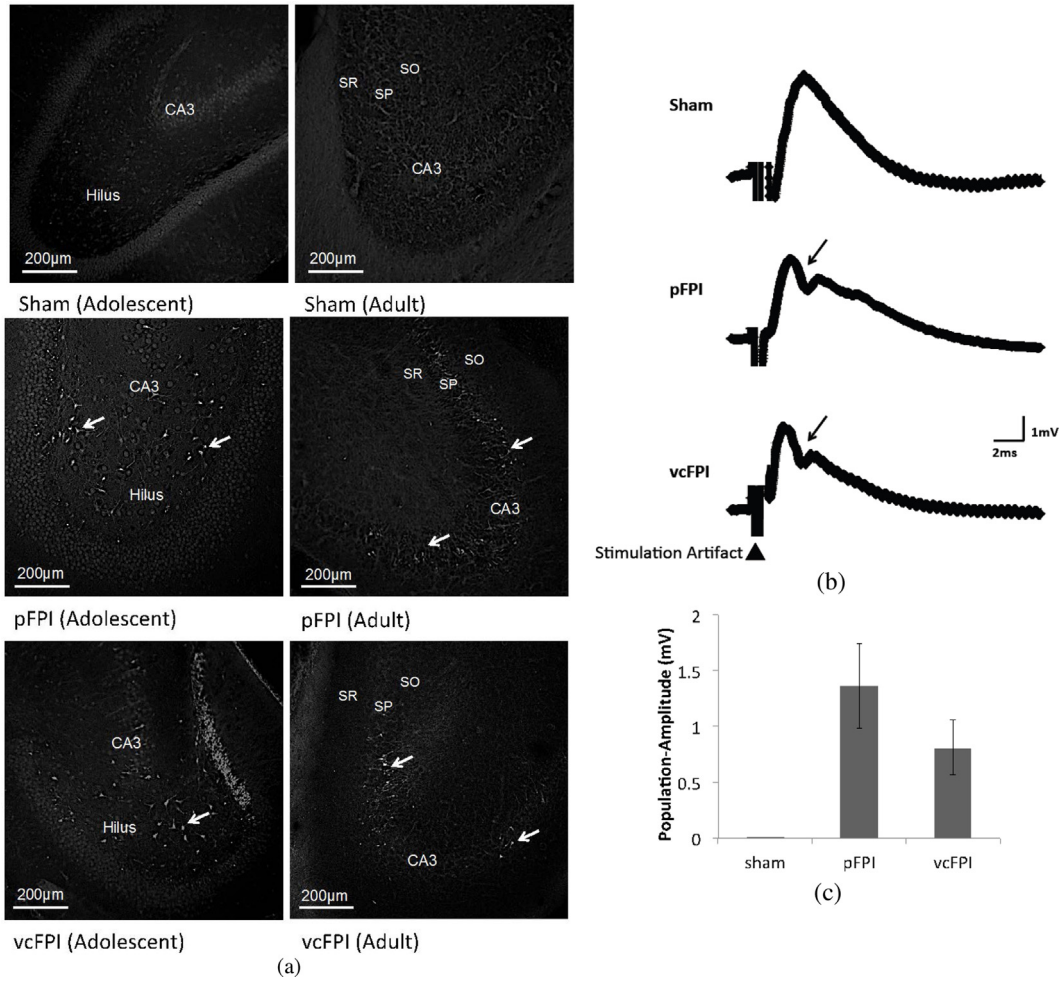

Fig. 7. Neurodegeneration and altered electrophysiological function. (a) Fluoro-Jade immunohistochemistry comparing sham, pFPI, and vcFPI. Arrows point to Fluoro-Jade positive neurons. (Left) Hippocampal slices show degenerating neurons in adolescent rats (4 h time point, horizontal brain tissue slices) and (right) adult rats (24 h time point, coronal brain tissue slices). (b) Electrophysiological studies 1-week post-injury (adolescent rats) showing similar enhancement in network excitability via similar population spike amplitude generation in pFPI and vcFPI. The granule cell population response was evoked by perforant path stimulation at 4 mA. Arrows point to population-spikes. (c) Average post-injury population amplitude. Error bars are SEM.

under different parameters of the fluid pressure waveform than percussions produced with the pendulum fluid percussion model (pFPI). Of particular interest is the ability to generate pressure waveforms with adjustable rise times in addition to peak pressures providing control over the impulse of the fluid percussion. This design enabled fluid percussions similar to the commonly used pFPI device as well as the ability to independently vary rise times and peak pressure.

4.1. Fluid percussion via motion control

The pFPI is an open system where impact with the hydraulic cylinder is adjusted with pendulum height. For the vcFPI system, proportional, integrative and differential (PID) control of a voice-coil linear motion actuator was used to directly control motion of the piston of the hydraulic cylinder. The system uses a closed feedback system of measured position to control the motion of the piston in the hydraulic cylinder to create a pressure pulse waveform with desired characteristics. For instance, this system controls the piston displacement to affect the peak pressure and controls the piston velocity to affect the rate of pressure rise. Furthermore, control of the duration of motion could also be realized by adjusting the return velocity of the piston to its original position. The result is the independent and reproducible control of the fluid percussion waveform with the ability to make fine adjustments to each parameter. Ultimately, voice coil control could also be used to generate more complex waveforms associated with different types of head injury. Fig. 8 illustrates a fluid percussion containing multiple oscillating pressure peaks that might be associated with blunt head impacts (Zhang et al., 2009).

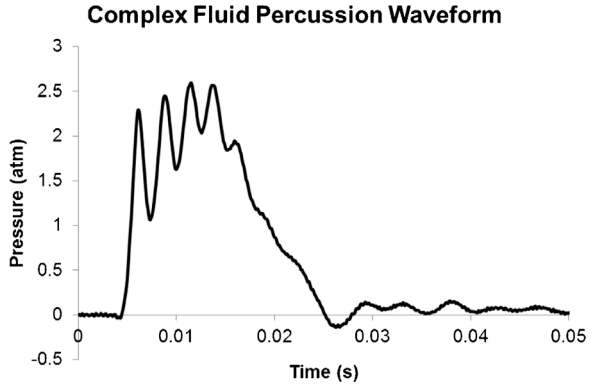

Fig. 8. Complex fluid percussion waveform containing multiple oscillating pressure peaks. This percussion has a similar maximum peak pressure and duration as a typically used fluid percussion (i.e. Fig. 4). The rise time is similar to the fast waveform and has four oscillating pressure peaks that may be more typical of a blunt head impact (Zhang et al., 2009).

Accurate and reproducible control of the voice-coil motion was shown in a closed system where the outlet valve was closed and did not allow for fluid to flow. Accurate and reproducible control was also achieved when the valve was open and no load attached (data not shown). This ensures that the system is operating properly and eliminates any variability in the motion from an attached load. Indeed, when the rat is attached there is an expected and profound effect on the output pressure waveform (Figs. 2 and 4). This is likely due to the fluid moving into the cranium and deforming brain tissue (Schettini and Walsh, 1988; Walsh et al., 1977; Walsh and Schettini, 1976). In addition, the fluid pressure could be affected by bulk movement of the fluid into other cranial compartments (Abbott, 2004; Schettini and Walsh, 1991). Both cases would require additional liquid to be injected from the FPI device into the cranium to raise the fluid percussion pressure. Interestingly, the irregularity of the fluid percussion waveform appears to be enhanced in the adolescent rat's cranium (Fig. 4) that is generally agreed to be softer and more compliant than the adult (Cheng et al., 2008; Elkin et al., 2010; Elkin and Morrison, 2013; Shulyakov et al., 2011). While not all studies agree brain stiffens with age (Levchakov et al., 2006), the difference in testing methods could lead to large discrepancies in results. In particular, the study of Shulyakov et al. (2011) is the most relevant to our experimental configuration where brain properties were tested in vivo with the meningeal compartments intact and is supported of the results of this study.

Both FPI systems have a small change in the slope of the rising phase (a small bump) and output pressure peaks that varies with the load. Since the relationship between fluid entering the cranium and deforming the brain tissues is most likely not linear, the fluid percussion waveform becomes irregular in comparison to the closed system. There is indeed a small drop in the peak pressure when an animal is attached vs. when no animal is attached, however this difference in the pFPI is smaller than the difference observed in the vcFPI system. During the pressure rising phase, additional fluid required to raise to fluid pressure due to intracranial deformations. For the vcFPI system, the hydraulic piston must move a greater distance. Accordingly, the irregularity in the slope of the pressure rise may also be in part due to the controller algorithm adjusting to pressure redistribution in the rat's cranium (Abbott, 2004; Schettini and Walsh, 1991; Shulyakov et al., 2011).

The experimenter typically compensates for differences in animals (i.e. differences in the load) by adjusting the height of the pendulum before the animal is injured. In the same way, the input displacement setting is altered to achieve the higher pressure in a vcFPI system. While we are convinced that these differences are based on the differences in the relative deformation within the cranium; we also suspect that part of the difference could arise from lab to lab differences in surgery, quality of the head cap connector and lab to lab FPI devices (the adult experiments were performed at a different lab from the adolescent experiments), or from the distance between the pressure sensor and the site of injury.

The variation in the load also has an effect on the applied pressure rise time. In the pFPI device, peak pressure was higher in adult animals compared to the adolescent animals while the rise time was lower in adult animals. This may be due to mechanical characteristics of the pendulum device. The inability to keep rise-time constant while changing the pressure peak, limits the pFPI device from isolating the pathophysiological outcome due to pressure differences from rise-time differences of injuries.

Tissues of the brain have viscoelastic behavior (Shuck and Advani, 1972; Cheng et al., 2008; Elkin and Morrison, 2013; Shulyakov et al., 2011; Pamidi and Advani, 1978; Wang and Wineman, 1972). At high rates of loading (peak pressure) viscoelastic materials behave stiffer and the magnitude of injury loading will induce higher stresses in the brain with lower amounts of deformation. On the other hand, at low rates of loading (same peak pressure) the brain will be more compliant with lower stresses and larger deformations. For instance, in the fast vcFPI injury, the rapid pressure pulse does not allow time for the brain tissue to deform resulting in an output pressure waveform is more similar to the operation with the valve closed. This device is the first of its kind that enables independent control over the rate and magnitude of the injury and can provide insight into how these parameters might influence pathophysiological outcomes.

4.2. Induction of fluid percussion injury

Here, we show that injury induced by the vcFPI system can reliably recreate a fluid percussion injury. The increase in righting time, response to toe pinch, seizure rate, mortality and Fluoro-Jade labeling of degenerating neurons in the hilus (4 h study) and CA3 hippocampus (24 h study) of pFPI injured rats compared to the sham group, is consistent with previous work using pFPI systems (Gupta et al., 2012; Zhao et al., 2003; Neuberger et al., 2014; Hallam et al., 2004; Zhong et al., 2005). We also see similar outcomes for injuries from the vcFPI device, which demonstrates that both the devices deliver similar injuries. This interpretation was supported by considering functional changes in dentate network excitability 1-week post TBI (Gupta et al., 2012; Santhakumar et al., 2001, 2003; Lowenstein et al., 1992; Toth et al., 1997). We have demonstrated a similar increase in dentate network excitability 1-week post TBI from both systems compared to sham.

4.3. Variability with rise-time, magnitude and impulse

Investigators studying neurophysiological outcomes at similar peak pressures can often encounter different results from lab to lab. This effect is typically considered to be variations in injury that arise from differences in the configuration of the fluid percussion device, variations between laboratories, and sometimes the experimenter. This study offers results that suggest differences in the fluid percussion waveform may be an important factor to differences in injury outcomes. With small increase in the rate of injury, immediate post injury indicators of injury may mask the underlying pathological severity that develops at a later stage (Neuberger et al., 2014). Also, the variability in the load (adult rat vs. adolescent rat) results in different pressure waveforms suggesting that injury may vary as well. This new vcFPI system will allow for investigations into these differences.

FPI studies typically relate the extent of histological damage associated with the severity/magnitude of the injury (i.e. peak pressure)(Cortez et al., 1989; Hicks et al., 1993, 1996; Lowenstein et al., 1992; Conti et al., 1998; Smith et al., 1991) as well as alterations in motor and sensory performance (Dixon et al., 1987; McIntosh et al., 1989; Lyeth et al., 1990; Hallam et al., 2004; Long et al., 1996; Pierce et al., 1998) and cognitive deficits (Lyeth et al., 1990; Hallam et al., 2004; Hicks et al., 1993; Smith et al., 1991; Schmidt et al., 1999). Here, we did an analysis of the mortality rate of a wider set of fluid percussion injuries to adult animals from a set of animals used for a different study in our lab. This mortality data set was not used in the other study. From the fluid percussion injuries performed, we observed that mortality from FPI is closely related to the rise time of injury. Furthermore, there were three surviving animals from our slow vcFPI injured animals that could not physically swim in the Morris water maze and were excluded from the behavioral experimentation of that study. We have not observed this phenomenon using the pFPI or fast vcFPI rise times of injury. Future work will need to be undertaken to investigate the effects of injury rate further.

Collectively our results suggest that this new voice coil model of TBI can be used to investigate the pathophysiology associated with varying rates of TBI. The mechanical response of

non-linear viscoelastic brain tissues to a low strain rate deformation will likely be different than its response to a high strain rate (Shuck and Advani, 1972; Elkin and Morrison, 2013; Pamidi and Advani, 1978). Systemic investigation of relevant loading parameters and the resulting responses are important for understanding injury-induced pathophysiological mechanisms and developing experimental models that are relevant to the human clinical situation under different types of head trauma. This variable rate voice coil fluid percussion injury device will help in deciphering the post traumatic sequel for different rate injuries, and for development of new treatment approaches by determining injury mechanisms across the temporal spectrum of the injury response.

Acknowledgement

This research was funded by the New Jersey Commission on Brain Injury Research, CBIR11PJT003.

References

Abbott NJ. Evidence for bulk flow of brain interstitial fluid: significance for physiology and pathology. Neurochem Int 2004;45(4):545–52.
Adams JH, Graham DI, Gennarelli TA. Head injury in man and experimental animals: neuropathology. Acta Neurochir Suppl (Wien) 1983;32:15–30.
Arbogast KB, Thibault KL, Pinheiro BS, Winey KI, Margulies SS. A high-frequency shear device for testing soft biological tissues. J Biomech 1997;30(7):757–9.
Cater HL, Sundstrom LE, Morrison B 3rd. Temporal development of hippocampal cell death is dependent on tissue strain but not strain rate. J Biomech 2005.
Cheng S, Clarke EC, Bilston LE. Rheological properties of the tissues of the central nervous system: a review. Med Eng Phys 2008;30(10):1318–37.
Conti AC, Raghupathi R, Trojanowski JQ, McIntosh TK. Experimental brain injury induces regionally distinct apoptosis during the acute and delayed post-traumatic period. J Neurosci 1998;18(15):5663–72.
Cortez SC, McIntosh TK, Noble LJ. Experimental fluid percussion brain injury: vascular disruption and neuronal and glial alterations. Brain Res 1989;482(2):271–82.
Dail WG, Feeney DM, Murray HM, Linn RT, Boyeson MG. Responses to cortical injury: II. Widespread depression of the activity of an enzyme in cortex remote from a focal injury. Brain Res 1981;211(1):79–89.
Dixon CE, Lyeth BG, Povlishock JT, Findling RL, Hamm RJ, Marmarou A, et al. A fluid percussion model of experimental brain injury in the rat. J Neurosurg 1987;67(1):110–9.
Elkin BS, Morrison B. Viscoelastic properties of the P17 and adult rat brain from indentation in the coronal plane. J Biomech Eng 2013;135(11):114507.
Elkin BS, Ilankovan A, Morrison B 3rd. Age-dependent regional mechanical properties of the rat hippocampus and cortex. J Biomech Eng 2010;132(1):011010.
Faul F, Xu L, Wald MM, Coronado VG. Traumatic brain injury in the United States: emergency department visits, hospitalizations and deaths 2002–2006. Atlanta, GA: Centers for Disease Control and Prevention, National Center for Injury Prevention and Control; 2010.
Feeney DM, Boyeson MG, Linn RT, Murray HM, Dail WG. Responses to cortical injury: I. Methodology and local effects of contusions in the rat. Brain Res 1981;211(1):67–77.
Ganpule S, Alai A, Plougonven E, Chandra N. Mechanics of blast loading on the head models in the study of traumatic brain injury using experimental and computational approaches. Biomech Model Mechanobiol 2013;12(3):511–31.
Graham DI, Raghupathi R, Saatman KE, Meaney D, McIntosh TK. Tissue tears in the white matter after lateral fluid percussion brain injury in the rat: relevance to human brain injury. Acta Neuropathol 2000;99(2):117–24.
Gupta A, Elgammal FS, Proddutur A, Shah S, Santhakumar V. Decrease in tonic inhibition contributes to increase in dentate semilunar granule cell excitability after brain injury. J Neurosci 2012;32(7):2523–37.
Hallam TM, Floyd CL, Folkerts MM, Lee LL, Gong QZ, Lyeth BG, et al. Comparison of behavioral deficits and acute neuronal degeneration in rat lateral fluid percussion and weight-drop brain injury models. J Neurotrauma 2004;21(5):521–39.
Hicks RR, Smith DH, Lowenstein DH, Saint Marie R, McIntosh TK. Mild experimental brain injury in the rat induces cognitive deficits associated with regional neuronal loss in the hippocampus. J Neurotrauma 1993;10(4):405–14.
Hicks R, Soares H, Smith D, McIntosh T. Temporal and spatial characterization of neuronal injury following lateral fluid-percussion brain injury in the rat. Acta Neuropathol 1996;91(3):236–46.
Hyder AA, Wunderlich CA, Puvanachandra P, Gururaj G, Kobusingye OC. The impact of traumatic brain injuries: a global perspective. NeuroRehabilitation 2007;22(5):341–53.
King AI, Yang KH, Zhang L, Hardy W, Viano DC. Is head injury caused by linear or angular acceleration? In: IRCOBI Conference; 2003.
Levchakov A, Linder-Ganz E, Raghupathi R, Margulies SS, Gefen A. Computational studies of strain exposures in neonate and mature rat brains during closed head impact. J Neurotrauma 2006;23(10):1570–80.
Liu YK, Chandran KB, von Rosenberg DU. Angular acceleration of viscoelastic (Kelvin) material in a rigid spherical shell-a rotational head injury model. J Biomech 1975;8(5):285–92.
Long JB, Gordon J, Bettencourt JA, Bolt SL. Laser-Doppler flowmetry measurements of subcortical blood flow changes after fluid percussion brain injury in rats. J Neurotrauma 1996;13(3):149–62.
Lowenstein DH, Thomas MJ, Smith DH, McIntosh TK. Selective vulnerability of dentate hilar neurons following traumatic brain injury: a potential mechanistic link between head trauma and disorders of the hippocampus. J Neurosci 1992;12(12):4846–53.
Lyeth BG, Jenkins LW, Hamm RJ, Dixon CE, Phillips LL, Clifton GL, et al. Prolonged memory impairment in the absence of hippocampal cell death following traumatic brain injury in the rat. Brain Res 1990;526(2):249–58.
Magou GC, Guo Y, Choudhury M, Chen L, Hususan N, Masotti S, et al. Engineering a high throughput axon injury system. J Neurotrauma 2011;28(11):2203–18.
Marmarou A, Foda MA, van den Brink W, Campbell J, Kita H, Demetriadou K. A new model of diffuse brain injury in rats. Part I: Pathophysiology and biomechanics. J Neurosurg 1994;80(2):291–300.
McIntosh TK, Vink R, Noble L, Yamakami I, Fernyak S, Soares H, et al. Traumatic brain injury in the rat: characterization of a lateral fluid-percussion model. Neuroscience 1989;28(1):233–44.
Meaney DF, Smith DH, Shreiber DI, Bain AC, Miller RT, Ross DT, et al. Biomechanical analysis of experimental diffuse axonal injury. J Neurotrauma 1995;12(4):689–94.
Morales DM, Marklund N, Lebold D, Thompson HJ, Pitkanen A, Maxwell WL, et al. Experimental models of traumatic brain injury: do we really need to build a better mousetrap? Neuroscience 2005;136(4):971–89.
Neuberger EJ, Abdul Wahab R, Jayakumar A, Pfister BJ, Santhakumar V. Distinct effect of impact rise times on immediate and early neuropathology after brain injury in juvenile rats. J Neurosci Res 2014;92(10):1350–61.
Pamidi MR, Advani SH. Nonlinear constitutive relations for human brain tissue. J Biomech Eng 1978;100:44–8.
Pfister BJ, Weihs TP, Betenbaugh M, Bao G. An in vitro uniaxial stretch model for axonal injury. Ann Biomed Eng 2003;31(5):589–98.
Pierce JE, Smith DH, Trojanowski JQ, McIntosh TK. Enduring cognitive: neurobehavioral and histopathological changes persist for up to one year following severe experimental brain injury in rats. Neuroscience 1998;87(2):359–69.
Santhakumar V, Ratzliff AD, Jeng J, Toth Z, Soltesz I. Long-term hyperexcitability in the hippocampus after experimental head trauma. Ann Neurol 2001;50(6):708–17.
Santhakumar V, Voipio J, Kaila K, Soltesz I. Post-traumatic hyperexcitability is not caused by impaired buffering of extracellular potassium. J Neurosci 2003;23(13):5865–76.
Sawauchi S, Marmarou A, Beaumont A, Tomita Y, Fukui S. A new rat model of diffuse brain injury associated with acute subdural hematoma: assessment of varying hematoma volume, insult severity, and the presence of hypoxemia. J Neurotrauma 2003;20(7):613–22.
Schettini A, Walsh EK. Brain tissue elastic behavior and experimental brain compression. Am J Physiol 1988;255(5 Pt 2):R799–805.
Schettini A, Walsh EK. Contribution of brain distortion and displacement to CSF dynamics in experimental brain compression. Am J Physiol 1991;260(1 Pt 2):R172–8.
Schmidt RH, Scholten KJ, Maughan PH. Time course for recovery of water maze performance and central cholinergic innervation after fluid percussion injury. J Neurotrauma 1999;16(12):1139–47.
Schmued LC, Hopkins KJ. Fluoro-Jade B: a high affinity fluorescent marker for the localization of neuronal degeneration. Brain Res 2000;874(2):123–30.
Shuck LZ, Advani SH. Rheological response of human brain tissue in shear. Trans ASME J Basic Eng 1972;12:905–11.
Shulyakov AV, Cenkowski SS, Buist RJ, Del Bigio MR. Age-dependence of intracranial viscoelastic properties in living rats. J Mech Behav Biomed Mater 2011;4(3):484–97.
Smith DH, Meaney DF. Axonal damage in traumatic brain injury. Neuroscientist 2000;6(6):483–95.
Smith DH, Okiyama K, Thomas MJ, Claussen B, McIntosh TK. Evaluation of memory dysfunction following experimental brain injury using the Morris water maze. J Neurotrauma 1991;8(4):259–69.
Smith DH, Chen XH, Xu BN, McIntosh TK, Gennarelli TA, Meaney DF. Characterization of diffuse axonal pathology and selective hippocampal damage following inertial brain trauma in the pig. J Neuropathol Exp Neurol 1997;56(7):822–34.
Sundaramurthy A, Alai A, Ganpule S, Holmberg A, Plougonven E, Chandra N. Blast-induced biomechanical loading of the rat: an experimental and anatomically accurate computational blast injury model. J Neurotrauma 2012;29(13):2352–64.
Thompson HJ, Lifshitz J, Marklund N, Grady MS, Graham DI, Hovda DA, et al. Lateral fluid percussion brain injury: a 15-year review and evaluation. J Neurotrauma 2005;22(1):42–75.
Toth Z, Hollrigel GS, Gorcs T, Soltesz I. Instantaneous perturbation of dentate interneuronal networks by a pressure wave-transient delivered to the neocortex. J Neurosci 1997;17(21):8106–17.
Walsh EK, Schettini A. Elastic behavior of brain tissue in vivo. Am J Physiol 1976;230(4):1058–62.
Walsh EK, Furniss WW, Schettini A. On measurement of brain elastic response in vivo. Am J Physiol 1977;232(1):R27–30.
Wang HC, Wineman AS. A mathematical model for the determination of viscoelastic behavior of brain in vivo. I. Oscillatory response. J Biomech 1972;5(5):431–46.

Yu J, Proddutur A, Elgammal FS, Ito T, Santhakumar V. Status epilepticus enhances tonic GABA currents and depolarizes GABA reversal potential in dentate fast-spiking basket cells. J Neurophysiol 2013;109(7):1746–63.
Zhang J, Yoganandan N, Pintar FA. Dynamic biomechanics of the human head in lateral impacts. Ann Adv Automotive Med/Annu Sci Conf 2009;53:249–56.
Zhao X, Ahram A, Berman RF, Muizelaar JP, Lyeth BG. Early loss of astrocytes after experimental traumatic brain injury. Glia 2003;44(2):140–52.
Zhong C, Zhao X, Sarva J, Kozikowski A, Neale JH, Lyeth BG. NAAG peptidase inhibitor reduces acute neuronal degeneration and astrocyte damage following lateral fluid percussion TBI in rats. J Neurotrauma 2005;22(2):266–76.